Quantifying the mesoscopic quantum coherence of approximate NOON states and spin-squeezed two-mode Bose-Einstein condensates

B. Opanchuk, L. Rosales-Zárate, R. Y. Teh and M. D. Reid
Centre for Quantum and Optical Science, Swinburne University of Technology, Melbourne, Australia

We examine how to signify and quantify the mesoscopic quantum coherence of approximate two-mode NOON states and spin-squeezed two-mode Bose-Einstein condensates (BEC). We identify two criteria that verify a nonzero quantum coherence between states with quantum number different by n. These criteria negate certain mixtures of quantum states, thereby signifying a generalised n-scopic Schrodinger cat-type paradox. The first criterion is the correlation $\langle \hat{a}^{\dagger n}\hat{b}^{n}\rangle \neq 0$ (here $\hat{a}$ and $\hat{b}$ are the boson operators for each mode). The correlation manifests as interference fringes in n-particle detection probabilities and is also measurable via quadrature phase amplitude and spin squeezing measurements. Measurement of $\langle \hat{a}^{\dagger n}\hat{b}^{n}\rangle$ enables a quantification of the overall n-th order quantum coherence, thus providing an avenue for high efficiency verification of a high-fidelity photonic NOON states. The second criterion is based on a quantification of the measurable spin-squeezing parameter ξ_N. We apply the criteria to theoretical models of NOON states in lossy interferometers and double-well trapped BECs. By analysing existing BEC experiments, we demonstrate generalised atomic "kitten" states and atomic quantum coherence with $n \gtrapprox 10$ atoms.

arXiv:1609.06028v2 [quant-ph] 7 Mar 2017

I. INTRODUCTION

In 1935 Schrodinger considered the preparation of a macroscopic system in a quantum superposition of two macroscopically distinguishable states [1]. Such systems are called "Schrodinger cat-states" after Schrodinger's example of a cat in a superposition of dead and alive states. The preparation of such states in the laboratory is difficult due to the existence of external couplings, which cause the superposition state to decohere to a classical mixture [2, 3]. While for the mixture the "cat" is probabilistically "dead" or "alive", the paradox is that for the superposition the "cat" is apparently neither "dead" or "alive". Developments in quantum optics and the cooling of atoms and mechanical oscillators have made the generation of mesoscopic cat-states feasible [4, 5]. This is interesting for atomic systems where a superposition of a massive system being in two states at different locations might be created. Ghirardi, Rimini, Weber [6] and Diosi [7] and Penrose [8] have proposed that for such systems decoherence mechanisms would prevent the formation of the Schrodinger cat superposition states. To carry out tests, firm proposals are required for the creation and detection of cat-states.

A major consideration for cat-state experiments is that the generation of the cat-state is not likely to be ideal. This is especially true for larger N. One of the most well-studied cat-states is the NOON state [9–14]

$$|\psi_{NOON}\rangle = \frac{1}{\sqrt{2}}\{|N\rangle_a|0\rangle_b + e^{i\phi}|0\rangle_a|N\rangle_b\} \tag{1}$$

where N particles or photons are superposed as being in the spatial mode a or the spatial mode b. Ideally, a cat-state requires $N \to \infty$ but "N-*scopic* kitten-state" realisations focus on finite $N > 1$. Here $|n\rangle_a$ ($|m\rangle_b$) are the eigenstates of particle number $\hat{n}_a = \hat{a}^\dagger\hat{a}$ ($\hat{n}_b = \hat{b}^\dagger\hat{b}$), respectively, and $\hat{a}$, $\hat{a}^\dagger$ ($\hat{b}$, $\hat{b}^\dagger$) are the boson operators for mode a (b). The NOON states have been generated in optics for N up to 5 [13] and with atoms for $N = 2$ [15]. At low N however photon detection efficiencies are usually very low and results are often obtained by postselection processes.

Generating for higher N is challenging. Proposals exist to exploit the nonlinear interactions formed from Bose Einstein condensates (BEC) trapped in the spatially separated wells of an optical lattice [16–24]. Under some conditions, theory shows that the atoms can tunnel between the wells, resulting in the formation of a NOON superposition. However, it is known that for realistic parameters, the states generated are in fact of the type

$$|\psi\rangle = \sum_{m=0}^{N} d_m|N-m\rangle_a|m\rangle_b \tag{2}$$

where there exist nonzero probabilities for numbers other than 0 or N [19, 21–23, 25]. (The d_m are probability amplitudes). Oscillation between two BEC states with significantly different mode numbers has been experimentally observed [26], presumably resulting in the formation of a superposition of type (2) at intermediate times.

A key question (raised by Leggett and Garg [27]) is how to rigorously signify the Schrodinger cat-like property of the state in such a non-ideal scenario. In this paper we propose quantifiable "catness" signatures that can be applied to nonideal NOON-type states generated in photonic and cold atom experiments. The signatures that we examine exclude *all classical mixtures* of sufficiently separated quantum states, so that it is possible to exclude all classical interpretations where the "cat" is "dead" *or* "alive" (see the Conclusion for a qualification). For the cat-system that can be found in one of two macroscopically distinguishable states ρ_D and ρ_A, a rigorous signature must negate *all* mixtures of the form

$$\rho_{mix} = P_D\rho_D + P_A\rho_A \tag{3}$$

where P_D and P_A are probabilities and $P_D + P_A = 1$. In our treatment, the ρ_D (ρ_A) are density operators for quantum states otherwise unspecified except that they give macroscopically distinct outcomes ("alive" or "dead") for a measurement of quantum number $\hat{n}_a - \hat{n}_b$.

The first step is to generalise this approach for the nonideal case (2), where there are nonzero probabilities for obtaining outcomes in an intermediate ("sleepy") domain over which the cat cannot be identified as either dead or alive. In Sections II and III, we follow Refs. [27, 29, 30] and consider states ρ_{DS} and ρ_{SA} that give outcomes in the combined "dead/ sleepy" and "sleepy/ alive" regions respectively. The states have overlapping outcomes indistinguishable over a range n. We explain how the negation of all mixtures of the type

$$\rho_{mix} = P_{-}\rho_{DS} + P_{+}\rho_{SA} \tag{4}$$

(where P_{-} and P_{+} are probabilities and $P_{-} + P_{+} = 1$) will imply a generalised n-scopic cat-type paradox, in the sense that the system cannot be explained by any mixture of quantum superpositions of states different by up to n quanta. It is proved that the observation of the nonzero n-scopic quantum coherence term

$$\langle 0|\langle n|\rho|0\rangle|n\rangle \neq 0 \tag{5}$$

(ρ is the density operator) will negate all mixtures of type (4), thus signifying a generalised n-scopic "kitten" quantum superposition. We identify two criteria that verify the n-scopic quantum coherence (5). In a separate paper, we examine a third criterion based on uncertainty relations and Einstein-Podolsky-Rosen steering [31].

Previous studies have proposed signatures (criteria or measures) for mesoscopic "cat" states (see for instance [3, 4, 22, 25, 29–39]). These include proposals based on interference fringes, entanglement measures, uncertainty relations, negative Wigner functions and state fidelity. Not all of these signatures however provide a direct negation of *all* the mixtures (3), (4). Further, most of these studies do not address the nonideal case where there may be a range of outcomes not binnable as either "dead" or "alive". Exceptions include the work of Refs. [22, 27, 29, 30, 32–35, 40] which (like the work of this paper) are based on the observations of a nonzero quantum coherence.

The first criterion that we consider is a nonzero *nth order correlation*

$$\langle \hat{a}^{\dagger n}\hat{b}^{n}\rangle \neq 0 \tag{6}$$

This criterion is necessary and sufficient for the nth order quantum coherence (5). While normally evidenced for NOON states by fringe patterns formed from n-fold photon count coincidences, we show in Section VII how this moment can also be measured for small N using highly efficient homodyne detection and Schwinger-spin moments. In Section IV, we show that the value of the coherence $\langle \hat{a}^{\dagger n}\hat{b}^{n}\rangle$ when suitably normalised translates to an *effective fidelity measure* of the n-scopic "catness" property of the state (which is not given directly by the state fidelity). We provide (in Section V) a theoretical model for the NOON state with losses, thus examining the degradation of the fidelity measure in that case. We also show how the fidelity measure can be applied to quantify mesoscopic quantum coherence for the case of number states $|N\rangle$ incident on a beam splitter (the *linear beam splitter* model). The quantum coherence (5) is optimally robust with respect to losses when $n \ll N$, but this can be achieved for high n.

The criterion (6) was proposed by Haigh et al to signify NOON-type superposition states created from nonlinear interactions in two-well BECs [22]. In Section VI, we evaluate $\langle \hat{a}^{\dagger n}\hat{b}^{n}\rangle$ in dynamical regimes suitable for the formation of approximate NOON states, using a two-mode Josephson model (the *nonlinear beam splitter*). In Section VII, we analyse the measurement strategy using multi-particle interferometry. For the case of $n = 2, 3$, the moment (6) is readily measured in terms of Schwinger spin observables. In fact by analysing spin squeezing data reported from the atomic BEC experiment of Esteve et al [41], we infer (in Section VIII) the existence of two-atom ($n = 2$) generalised (sometimes called "embedded" [21]) kitten-states.

The second criterion that we consider for an n-scopic quantum coherence (5) is based on *spin squeezing* [42, 43]. The amount of squeezing observed for a given number of atoms N is quantified by a squeeze parameter $\xi_N < 1$ [41, 44–46]. In Section IIIb, we apply the methods of Ref. [30] and prove that a given measured amount of squeezing places a lower bound of $\frac{\sqrt{N}}{\xi_N}$ on the value of n for which the quantum coherence $\langle 0|\langle n|\rho|0\rangle|n\rangle$ is nonzero:

$$n > \frac{\sqrt{N}}{\xi_N} \tag{7}$$

This criterion requires $\langle \hat{a}^{\dagger}\hat{b}\rangle \neq 0$ and is not therefore useful to identify ideal NOON states. However the squeezing signature (7) is very effective in confirming a high degree of mesoscopic quantum coherence for states (2) where adjacent d_m and d_{m+1} are nonzero. This occurs in systems with high losses or linear couplings. In Section IIIb we apply this signature to published experimental data, and confirm a mesoscopic coherence (with $n \sim 10$ atoms) in two-mode BEC systems. We note this is consistent with the recent work of Ref. [32, 35] which proposes *quantifiers (measures)* of mesoscopic quantum coherence based on Fisher information and reports significant values of atomic coherence for BEC systems.

II. n-SCOPIC QUANTUM COHERENCE

We begin by considering the outcomes of observable $2\hat{J}_Z = (\hat{a}^{\dagger}\hat{a} - \hat{b}^{\dagger}\hat{b})$. For the ideal NOON state (1) these are $-N$ and N. In the limit of large N, we identify the two outcomes as "dead (D)" and "alive (A)" in order to make a simplistic analogy with the Schrodinger cat example. How does one signify the superposition nature of the NOON state? The density matrix ρ for the superposition $|\psi_{NOON}\rangle$ has nonzero off-diagonal coherence terms $\langle 0|\langle N|\rho|0\rangle|N\rangle \neq 0$ that distinguish it from the classical mixture (P_D and P_A are probabilities, $P_D + P_A = 1$)

$$\rho_{mix} = P_D|0\rangle|N\rangle\langle N|\langle 0| + P_A|N\rangle|0\rangle\langle 0|\langle N| \tag{8}$$

Thus, the detection of the nonzero coherence $\langle 0|\langle N|\rho|0\rangle|N\rangle$ serves to signify an N-scopic cat-state in this case.

The ultimate objective of a "Schrodinger cat" experiment is to negate classical realism at a macroscopic level. The accepted definition of **macroscopic realism** is that a system must be in a classical mixture of two macroscopically distinguishable states [27]. Similarly, we take as the definition of N**-scopic realism** is that a system must be in a classical mixture of two states that give predictions different by N quanta. In this paper, the meaning of *classical mixture* is in the *quantum* sense only, that the density operator ρ for the system is equivalent to a classical mixture of the two (quantum) states, as in (8).

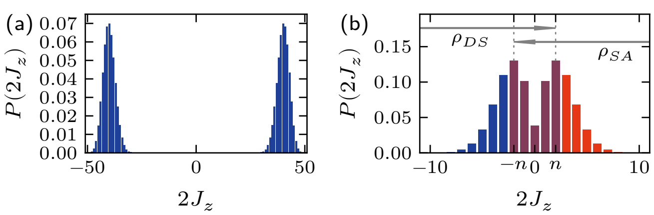

Figure 1: *Nonideal scenarios for NOON generation:* Probability $P(2j_z)$ of an outcome of $2\hat{J}_z$ for the NOON state after attenuation as modelled by a beam splitter coupling. (a) $N = 50$, $\eta = 0.8$ (b) $\eta = 0.05$. Similar plots are obtained for pure NOON-type states (2) generated via a Josephson two-mode interaction. The right graph shows how to confirm an n-scopic quantum coherence, as explained in the text.

More generally, the states generated in the experiments give outcomes for $\hat{n}_a$ and $\hat{n}_b$ different to 0 and N, as a result of even a small amount of loss or noise in the system (real predictions are illustrated in Figure 1). The question becomes how to confirm by experiment that the system is indeed in a superposition of two mesoscopically distinguishable quantum states, as opposed to any alternative classical description where there would be no mesoscopic "cat" paradox. This question was examined in Ref. [29, 30] for continuous outcomes realised from quadrature phase amplitude measurements and we apply the approach given there. The following is a result found in that paper as applied to this case.

Result 1:− **An** ***n-scopic quantum coherence and generalised n-scopic cat-paradox*****:** Consider the following mixture sketched in Figure 1b (for $j_c = 0$).

$$\rho_{mix} = P_-\rho_{DS} + P_+\rho_{SA} \tag{9}$$

where P_- and P_+ are probabilities and $P_- + P_+ = 1$. Here, ρ_{DS} is a quantum state whose two-mode number state expansion may only include eigenstates with outcome $2J_z < j_c + n$; and ρ_{SA} is a quantum state whose expansion only includes eigenstates with $2J_z > j_c - n$. The outcome $2J_z \geq j_c + n$ is interpreted as "alive" and the outcome $2J_z \leq j_c - n$ is interpreted as "dead". The intermediate overlapping regime is "sleepy". The negation of all mixtures of the type (9) will imply a generalised n-scopic "cat-type" paradox, in the sense that the system cannot be viewed as either "dead/ sleepy" or "alive/ sleepy"− and cannot therefore be explained by any mixture of superpositions of states different by up to n quanta. If (9) can be negated, then there is an n-*scopic generalised quantum coherence (cat-type paradox).* The negation of (9) implies that for some n', m'

$$_b\langle n + m'|_a\langle n'|\rho|n + n'\rangle_a|m'\rangle_b \neq 0 \tag{10}$$

(in fact $j_c = n' - m'$). The converse is also true. Conditions that negate (9) equivalently demonstrate (10), and we refer to these conditions as signatures of n- scopic quantum coherence, or of an n-scopic generalised cat paradox.

Proof: The justification is that if (9) fails, then the system cannot be thought of as being in one quantum state ρ_1 *or* the other ρ_2. We have not constrained the ρ_1 or ρ_2, except to say they cannot include both "dead" and "alive" states (each one is orthogonal to either the dead or alive state). Hence there is a negation of the premise that the system must always be either " dead or alive". In that sense we have an analogy with the Schrodinger "cat" paradox but where the "dead" and "alive" states are separated by n quanta. That the coherence is nonzero follows on expanding the density matrix in the number state basis. $\square$

We note that the nonzero n-scopic quantum coherence has a physical significance, in that it is then possible (in principle) to filter out the intermediate "sleepy states" using measurements of $|\hat{J}_Z| > n/2$ to create a conditional cat-state where the separation in J_Z of the "dead" and "alive" states is of order n. This method of preparation has been carried out experimentally [10]. However, where the n-scopic coherences are small, the heralding probability for the cat-state also becomes small, making the states increasingly difficult to generate. This motivates Section V which examines how to quantify the quantum coherence through experimental signatures. First, we identify two criteria for the condition Eq. (10).

III. TWO CRITERIA FOR n-SCOPIC QUANTUM COHERENCE

A. Correlation test

It is well known that higher order correlations can detect NOON states. We clarify with the following result.

Result 2:− ***The n-th order correlation test:*** Restricting to two-mode quantum descriptions for ρ, the observation of

$$\langle \hat{a}^{\dagger n}\hat{b}^{n}\rangle \neq 0 \tag{11}$$

is a signature of the n-scopic quantum coherence (10).

The Result can be proved straightforwardly by expanding the operator $\hat{a}^{\dagger n}\hat{b}^{n}$ in terms of the Fock basis elements $|n_a\rangle|n_b\rangle\langle m_b|\langle m_a|$ or equivalently by considering an arbitrary density matrix ρ written in the two-mode Fock basis and noting that the condition (11) is equivalent to (10). We will find it useful to note the following: If the moment $\langle \hat{a}^{\dagger n}\hat{b}^{n}\rangle$ is nonzero then there is a nonzero probability that the system is in the following *generalised n-scopic superposition* state:

$$\begin{aligned}|\psi_n\rangle \;&=\; a^{(n)}_{n'm'}|n'\rangle|m'+n\rangle + b^{(n)}_{n'm'}|n'+n\rangle|m'\rangle \\ &\quad + d|\psi_0\rangle \end{aligned}\tag{12}$$

The $a^{(n)}_{n'm'}, b^{(n)}_{n'm'}, d$ are probability amplitudes satisfying $a^{(n)}_{n'm'}, b^{(n)}_{n'm'} \neq 0$, the d being unspecified. $|\psi_0\rangle$ is an unspecified quantum state orthogonal to the states $|n'\rangle|m'+n\rangle$ and $|n'+n\rangle|m'\rangle$. The meaning of "nonzero probability that the system is in" in this context is that the density operator for the quantum system is *necessarily* of the form $\rho = \sum_R P_R|\psi_R\rangle\langle\psi_R|$ where at least one of the states $|\psi\rangle_R$ with nonzero P_R is an n-scopic superposition state $|\psi_n\rangle$. The Appendix A gives a detailed explanation of this last result.□

B. Spin squeezing test and application to experiment

Significant nth order quantum coherence can also in some cases be detected by observation of spin squeezing. We define the standard Schwinger operators

$$\begin{aligned}\hat{J}_X \;&=\; \left(\hat{a}^{\dagger}\hat{b} + \hat{a}\hat{b}^{\dagger}\right)/2 \\ \hat{j}_Y \;&=\; \left(\hat{a}^{\dagger}\hat{b} - \hat{a}\hat{b}^{\dagger}\right)/(2i) \\ \hat{J}_Z \;&=\; \left(\hat{a}^{\dagger}\hat{a} - \hat{b}^{\dagger}\hat{b}\right)/2 \\ \hat{N} \;&=\; \hat{a}^{\dagger}\hat{a} + \hat{b}^{\dagger}\hat{b}\end{aligned}\tag{13}$$

We consider a system described by a superposition of two-mode number states as in (2). Thus we specify a generalised superposition as

$$\begin{aligned}|\psi\rangle \;&=\; \sum_{i,j} c_{ij}|n_i\rangle|m_j\rangle \\ &\equiv\; \sum_k d_k|\psi_k\rangle\end{aligned}\tag{14}$$

where the last line relabels (for convenience) all states of the ij array by an index k. In (2) we have a superposition $|\psi\rangle = \sum_{n=0} d_n|n\rangle|N-n\rangle$ where N (the total number of particles) is fixed. This case for large N and where $d_n \neq 0$ for some $n \neq 0, N$ has been described as a superposition of "dead", "alive" and "sleepy" cats. Considering the general case (14), we can define for each term $|\psi_k\rangle$ such that $d_k \neq 0$ the spin number difference $j_k = (n_i - m_j)/2$. The aim is to put a lower bound on the spread of possible j_k values (depicted in Figure 1). We define the spread as

$$\delta = max\{|j_k - j_{k'}|\} \tag{15}$$

such that for j_k and $j_{k'}$, the coefficients d_k, $d_{k'} \neq 0$. For the ideal NOON state, $\delta = N$. Here max denotes the maximum of the set.

We can show that a certain amount of squeezing in J_Y determines a lower bound in the spread of eigenstates of J_Z. The method is similar to that given in Ref. [30] which studied quadrature phase amplitude squeezing. The spin Heisenberg uncertainty relation is

$$(\Delta\hat{J}_Y)(\Delta\hat{J}_Z) \geq |\langle\hat{J}_X\rangle|/2 \tag{16}$$

Spin squeezing is obtained when [42, 43]

$$(\Delta\hat{J}_Y)^2 < |\langle\hat{J}_X\rangle|/2 \tag{17}$$

It is clear that in that case a low variance $(\Delta\hat{J}_Y)^2$ will always imply a high variance in $\hat{J}_Z$. For many spin squeezing experiments, $\langle\hat{J}_X\rangle \sim \langle\hat{N}\rangle/2$ which means the Bloch vector lies on the surface or near the surface of the Bloch sphere, so that the system is close to a pure state. Squeezing is then obtained when $(\Delta\hat{J}_Y)^2 < \langle\hat{N}\rangle/4$.

For pure states, the high variance in $\hat{J}_Z$ is associated with a minimum spread of the superposition of eigenstates of $\hat{J}_Z$. Thus, there is a lower bound on the best amount of squeezing determined by the maximum spread (extent) δ of the superposition. In the Appendix, following the methods of Refs. [30], this connection is generalised for mixed states. We prove the following result.

Result 3:– ***Spin squeezing test for n-th order quantum coherence:*** An experimentally measured amount of spin squeezing in J_Y is defined in terms of a "squeezing parameter"

$$\xi_N = \frac{\left(\Delta\hat{J}_Y\right)}{\sqrt{|\langle\hat{J}_X\rangle|/2}} \rightarrow \frac{\left(\Delta\hat{J}_Y\right)}{\langle N\rangle^{1/2}/2} \tag{18}$$

where $\xi_N < 1$ implies spin squeezing and $\xi_N = 0$ is the optimal possible squeezing (achievable as $N \rightarrow \infty$). Here we have taken the case where $\langle\hat{J}_X\rangle \sim \langle\hat{N}\rangle/2$. We can conclude that there exists a nonzero coherence $\langle 0|\langle n|\rho|0\rangle|n\rangle \neq 0$ for a value n where

$$n > \frac{\sqrt{N}}{\xi_N} \tag{19}$$

Proof: The proof is given in the Appendix. □

The particular test given by Result 3 requires $\langle\hat{J}_X\rangle \neq 0$. This would imply nonzero single atom coherence terms given as $\langle \hat{a}^\dagger \hat{b} \rangle \neq 0$. We note that the final result (19) indicates that the coherence size is of order $\sqrt{N}$. Spin squeezing with a considerable number N of atoms has been observed in several atomic experiments and excellent agreement has been obtained for $N \sim 100$ with a two-mode model [41, 44, 45]. Typically, the number of atoms is $N \sim 100$ or more, indicating values of quantum coherence of order $n > 10$ atoms.

IV. MEASURABLE QUANTIFICATION OF THE MESOSCOPIC QUANTUM COHERENCE

A. Catness fidelity and quantum coherence

The observation of $\langle \hat{a}^{\dagger n} \hat{b}^n \rangle \neq 0$ certifies the existence of the (nonzero) n-scopic quantum coherence, but does not specify the *magnitude* of the quantum coherence (QC), originating from terms like

$$C_n^{(n',m')} = 2|_b\langle n+m'|_a\langle n'|\rho|n+n'\rangle_a|m'\rangle_b| \qquad (20)$$

taken from Eq. (10). In fact, we can easily identify states (such as $|\alpha\rangle|\beta\rangle$) for which the n-scopic quantum coherence vanishes as $n \to \infty$ (for any m', n'), but for which the moment $\langle \hat{a}^{\dagger n} \hat{b}^n \rangle$ increases. Put another way, the observation $\langle \hat{a}^{\dagger n} \hat{b}^n \rangle \neq 0$ does not tell us the probability P_R that the system will be found in an associated n-scopic superposition Eq. (12), nor the values of the probability amplitudes $a_{n'm'}^{(n)}$,$b_{n'm'}^{(n)}$.

We explain in this Section that the measured correlation $\langle \hat{a}^{\dagger n} \hat{b}^n \rangle$ *when suitably normalised* places a lower bound on the sum of the magnitudes of the nth order quantum coherences, defined as

$$C_n = \mathcal{N} \sum_{n',m'} C_n^{(n',m')} \qquad (21)$$

Here $\mathcal{N}$ is a normalisation factor that ensures the maximum value of $C_n = 1$ for the optimal case. The normalised correlation thus gives measurable information about C_n which is an effective "*catness-fidelity*".

The "catness-fidelity" contrasts with the standard state-fidelity measure F (defined as the overlap between an experimental state ρ_{exp} and the desired superposition state [47]). The standard measure is not directly sufficient to quantify a cat-state since it may be possible for mixtures that are not cat-type superpositions to give a high absolute F as $N \to \infty$ [3].

B. General Result for two-mode mixed states

Defining a suitable catness-fidelity is straightforward for pure states. Any two-mode state $|\psi\rangle$ can be expanded in the number state basis and can thus be written in terms of a superposition of the states (12) but with $a_{n'm'}^{(n)}$, $b_{n'm'}^{(n)}$ arbitrary. The state fidelity F of $|\psi\rangle$ with respect to the symmetric n-scopic superposition

$$|\psi_{sup}\rangle \; = \; (|n'\rangle|m'+n\rangle + e^{i\phi}|n'+n\rangle|m'\rangle)/\sqrt{2}$$

is

$$\begin{aligned} F \; &= \; |\langle \psi_{\text{sup}}|\psi\rangle|^2 \\ &= \; \frac{1}{2}\left(|a_{n'm'}^{(n)}|^2 + |b_{n'm'}^{(n)}|^2 + 2|a_{n'm'}^{(n)} b_{n'm'}^{(n)*}|\right) \end{aligned} \qquad (22)$$

where the phase ϕ is chosen to maximise F. We see that the magnitude of the quantum coherence of the pure state density operator with respect to the states $|n'\rangle|m'+n\rangle$ and $|n'+n\rangle|m'\rangle$ is directly related to the fidelity F:

$$\begin{aligned} C_n^{(n',m')} \; &= \; 2|\langle m'+n|\langle n'|\rho|n+n'\rangle|m'\rangle| \\ &= \; 2|a_{n'm'}^{(n)} b_{n'm'}^{(n)*}| \end{aligned} \qquad (23)$$

We note that $F = 1$ if and only if $a_{n'm'}^{(n)} b_{n'm'}^{(n)*} = 1/2$, which implies $C_n^{(n'm')} = 1$. Similarly, $C_n^{(n',m')} = 1$ implies $F = 1$. An arbitrary two-mode pure state is a superposition of states over *different* n', m' and we may define as the total "n-scopic catness fidelity" the sum of the magnitudes of the nth order coherences i.e.

$$C_n \; = \mathcal{N} \textstyle\sum_{n',m'} C_n^{(n',m')} \; = \; 2\mathcal{N} \displaystyle\sum_{n',m'} |a_{n'm'}^{(n)} b_{n'm'}^{(n)*}| \qquad (24)$$

where $\mathcal{N}$ is a normalisation factor to ensure the maximum value of $C_n = 1$. A pure two-mode state with fixed N as given in the Introduction can be written

$$\begin{aligned} |\psi\rangle \; &= \; \sum_{m=0}^{N} d_m |N-m\rangle_a |m\rangle_b \\ &= \; \sum_{m'<N/2} d_{m'+n}|m'\rangle|m'+n\rangle + d_m|n+m'\rangle|m'\rangle \end{aligned} \qquad (25)$$

(The simplification in the last line is written for N odd.) The $a_{n'm'}^{(n)}$ and $b_{n'm'}^{(n)}$ can then be given in terms of $d_{m'+n}$ and $d_{m'}$. For a pure state, we see that C_n can be inferred from the probabilities for the mode number. However, this is not useful for the practical case of mixtures.

With this motivation, we note that the catness-fidelity C_n can be expressed in terms of the measurable higher order moments.

$$\langle \hat{a}^{\dagger n} \hat{b}^n \rangle \; = \; \sum_{n',m' \geq 0} a_{n'm'}^{(n)} b_{n'm'}^{(n)*} \sqrt{\frac{(m'+n)!}{m'!}} \sqrt{\frac{(n'+n)!}{n'!}} \qquad (26)$$

For a general two-mode state, using that $\langle \hat{a}^{\dagger n} \hat{b}^n \rangle =$

$Tr(\rho a^{\dagger n}b^n)=\sum_{n_a,m_b}\langle n_a|\langle m_b|\rho a^{\dagger n}b^n|n_a\rangle|m_b$, we find

$$\langle\hat{a}^{\dagger n}\hat{b}^{n}\rangle = \sum_{n',m'\geq 0}\sqrt{\frac{(n'+n)!}{n'!}}\sqrt{\frac{(m'+n)!}{(m')!}} \times\langle n'|\langle m'+n|\rho|n'+n\rangle|m'\rangle \tag{27}$$

This allows us to deduce the following general result.

Result** 4:– **Measurable lower bound estimate to the n-scopic "catness fidelity", defined as the sum of the magnitudes of nth order quantum coherences:

The measurable quantity

$$c_n=\frac{2|\langle\left(\hat{a}^{\dagger}\right)^{n}\hat{b}^{n}\rangle|}{S} \tag{28}$$

gives a *lower bound* to the true catness-fidelity C_n. Here $S=sup_{n',m'}\{\sqrt{\frac{(m'+n)!}{m'!}}\sqrt{\frac{(n'+n)!}{n'!}}\}$ over values of n', m' satisfying that the probability $P_{m',n'+n}$ for detecting m' and $n'+n$ particles in modes b and a is nonzero, and also that the probability $P_{m'+n,n'}$ for detecting $m'+n$ and n' particles in modes b and a is nonzero.

Proof: The proof follows from (27) using the definition (21). □ Realistically, it is difficult in an experiment to truly verify that the probability for obtaining a certain mode number is zero. In light of this, we deduce in the Appendix C a correction term to the Result 4, assuming the experimentalist is at least able to verify that the "non-relevant" probabilities $P_{m',n'+n}$, $P_{m'+n,n'}$ are sufficiently small, and that there is a practical upper bound to the mode numbers (defined by an energy or atom number bound).

C. Ideal NOON case

In the ideal NOON case, an experimentalist would observe N particles in mode a or N particles in mode b. Consider an experiment where indeed only such probabilities are nonzero. This is not unrealistic for photonic experiments with small N that use postselection. The experimentalist could deduce that the most general form of the density operator in this case is

$$\rho=P_N\rho_N+P_{alt}\rho_{alt} \tag{29}$$

where ρ_N is the density operator of a NOON superposition (12) (with $n'=m'=d=0$), and ρ_{alt} is an alternative density operator describing classical mixtures of number states (namely $|N\rangle|0\rangle$ and $|0\rangle|N\rangle$). Here, $P_N+P_{alt}=1$ and P_N, P_{alt} are probabilities.

We see from (12) that the quantity C_N defined as

$$C_N=2|a_{00}^{(N)}b_{00}^{(N)}|P_N \tag{30}$$

gives an *effective fidelity measure* of the state ρ relative to the NOON cat state. We call the quantity C_N the *catness-fidelity*, and note that $0\leq C_N\leq 1$. Clearly, the value of $C_N=1$ is optimal and can only occur if the system ρ is the pure symmetric NOON state (1) for which $|a_{00}^{(N)}|=|b_{00}^{(N)}|=\frac{1}{\sqrt{2}}$. For the ideal NOON state, the prediction is $\langle a^{\dagger n}b^n\rangle=\delta_{Nn}N!/2$ and $S=N!$ so that the catness fidelity is indeed 1:

$$c_N=C_N=\frac{2}{N!}|\langle\left(a^{\dagger}\right)^{n}b^{n}\rangle|=1 \tag{31}$$

The value of C_N reduces for asymmetric NOON states or for mixed states where $P_N<1$.

V. EXAMPLES OF QUANTIFICATION

A. Attenuated NOON states

Photonic NOON states have been reported experimentally for up to $N=5$. For a rigorous detection of a cat-like state, it is necessary to account for losses that may arise as a result of processes including detection inefficiencies. To model loss, we use a simple beam splitter approach [3]. We calculate the moments of final detected fields $\hat{a}_{det}$, $\hat{b}_{det}$ given by $a_{det}=\sqrt{\eta}a+\sqrt{1-\eta}a_v$, $b_{det}=\sqrt{\eta}b+\sqrt{1-\eta}b_v$ where $\hat{a}$, $\hat{b}$ are the boson operators for the incoming field modes, prepared in a NOON state, and a_v, b_v are boson operators for vacuum modes associated with the environment. Here η is the probability that an incoming photon/ particle is detected. We find

$$\langle\hat{a}_{det}^{\dagger n}\hat{b}_{det}^{n}\rangle=\eta^n\langle\hat{a}^{\dagger n}\hat{b}^{n}\rangle=\eta^n\delta_{nN}N!/2 \tag{32}$$

The system is a mixture of type $\rho=P_N\rho_N+P_{alt}\rho_{alt}$ defined in (29). The catness-fidelity signature C_N of Eq. (29) is measurable as c_N ($S=N!$) defined by (28) and is plotted in Figure 2. Comparing with the distributions of Figure 1 which are generated for the attenuated NOON state, we see that only the extremes $n=N$ have a nonzero coherence. As loss increases, the Nth quantum coherence remains (in principle) rigorously certifiable since it is predicted that $\langle\hat{a}^{\dagger N}\hat{b}^{N}\rangle\neq 0$ for all values η. However, the fidelity C_N is greatly reduced with decreasing η, particularly for larger N (Figure 2).

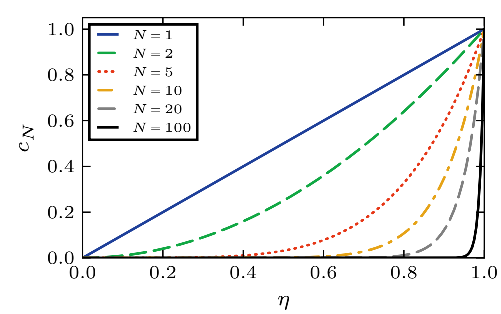

Figure 2: The Nth order catness-fidelity C_N (Eq. (30)) for the attenuated NOON state versus detection efficiency η. Here $C_N=c_N=2\langle\hat{a}^{\dagger n}\hat{b}^{n}\rangle/N!$. c_n and $\langle\hat{a}^{\dagger n}\hat{b}^{n}\rangle=0$ for $n<N$.

B. States formed from number states incident on a linear beam splitter

Next we consider a two-mode number state $|N\rangle|0\rangle$ incident at the two single-mode input ports of a beam splitter, so that N quanta are incident on one arm only. The output state is the N-scopic superposition (2) but with binomial coefficients:

$$|out\rangle \;=\; \sum_{m=0}^{N} d_m|m\rangle_a|N-m\rangle_b\,, \qquad (33)$$

where $d_m = \sqrt{N!}/\sqrt{2^N m!(N-m)!}$. Different to the NOON states, nonzero quantum coherences $\langle \hat{a}^{\dagger m}\hat{b}^m\rangle \neq 0$ exist for all $m \leq N$.

Evaluation gives that the pure state n-scopic catness-fidelity (24) (defined as the sum of the magnitude of all the nth order coherences) is

$$C_n = \mathcal{N}_{n,N}\sum_{m=0}^{N-n}|d_m d^*_{m+n}| \qquad (34)$$

where $\mathcal{N}_{n,N}$ is a normalisation constant to ensure the maximum value of C_n is 1. For this system, the normalisation $\mathcal{N}_{n,N}$ is determined by the bounds on the coherences of the density matrix for a pure state. For example, where $n = N$, $d_0 d^*_N \leq 1/2$ and hence $\mathcal{N}_{N,N} = 2$. The general results for the normalisation $\mathcal{N}_{n,N}$ are given in the Appendix C. Using Result 4, a measurable lower bound to the catness-fidelity given by (28) is

$$c_n = \frac{\mathcal{N}_{n,N}|\langle a^{\dagger n}b^n\rangle|}{S} \qquad (35)$$

where $S = max\{B_m^{(N,n)}\}$ (for N fixed) with

$$B_m^{(N,n)} \;=\; \sqrt{\frac{(m+n)!\,(N-m)!}{m!\,(N-m-n)!}}$$

The value of m that gives the maximum value of $B_m^{(N,n)}$ is given by: $m = (N-n)/2$ if N and n have the same parity, and $m = (N-n\pm 1)/2$ if n and N does not have the same parity.

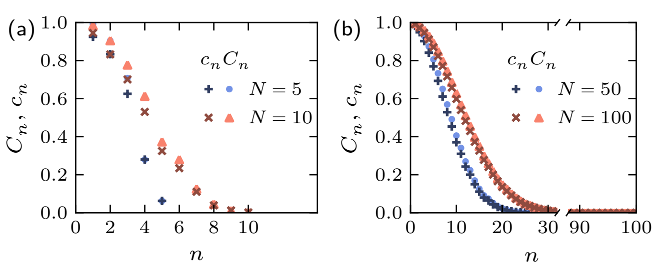

Figure 3: Measures of n-th order quantum coherence (catness-fidelity) for the output state of the linear beam splitter with N particles incident in one arm. C_N and c_n vs n, for $N = 5$, 10 and 100. $C_n \geq c_n$ as expected.

The expression S can be determined from the values of N, m, n which are known for the experiment. One can then experimentally measure the moment $\langle \hat{a}^{\dagger n}\hat{b}^n\rangle$ to obtain a value for c_n. The prediction is

$$\langle \hat{a}^{\dagger n}\hat{b}^n\rangle \;=\; \sum_{m=0}^{N-n} d^*_{m+n}d_m B_m^{(N,n)} \;=\; \frac{N!}{2^n(N-n)!} \qquad (36)$$

A comparison is given between the actual catness-fidelity C_n and the estimated one c_n in Figure 3 for this beam splitter case. We see that in this instance the lower bound is a good estimate of the actual fidelity. As might be expected for this system, the first order quantum coherence is significant whereas the highest order coherence given by $n = N$ is small. In fact all values of fidelity for $n > N/2$ are insignificant. We also note that for a fixed n, a higher fidelity can be obtained by increasing N to be much greater than n.

With attenuation present for each mode (as described in the previous section), we evaluate the final detected moments. The solutions are $\langle \hat{a}^{\dagger n}_{det}\hat{b}^n_{det}\rangle = \eta^n\langle \hat{a}^{\dagger n}\hat{b}^n\rangle$ where $\langle \hat{a}^{\dagger n}\hat{b}^n\rangle$ is given by (36). The density matrix has the same dimensionality as without losses, and the bounds on the coherences and the normalisation $\mathcal{N}_{n,N}$ are as above. Figure 4 plots the values of the catness-fidelity c_n versus efficiency η. We note that the first order coherence $n = 1$ is much more robust with respect to loss, as compared to the higher order coherences. Interesting is that for a fixed n, the robustness with respect to loss improves quite dramatically if one increases the value of N. At high N, the highest order coherences are almost immeasurable e.g. for $N = 100$, the quantum coherence becomes measurable at $n < 20$. We note also that the cut-off for a measurable n increases with increasing N, making generation of n-scopic cat-states in this generalised sense quite feasible.

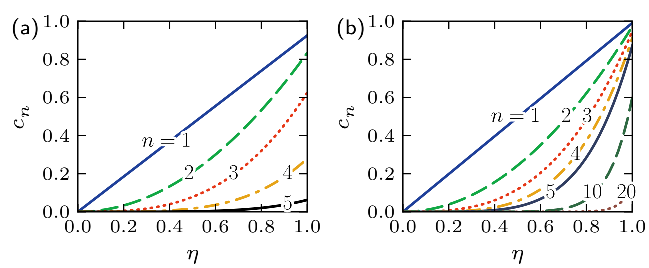

Figure 4: Measures of nth order quantum coherence (catness-fidelity) for the output of the linear beam splitter versus detection efficiency η. Definitions as for Figure 3. Left $N = 5$, Right $N = 100$.

VI. MESOSCOPIC QUANTUM COHERENCE IN DYNAMICAL TWO-WELL BOSE-EINSTEIN CONDENSATES

A. Hamiltonian and Model

A mesoscopic NOON state can in principle be created from the nonlinear interaction modelled by the two-mode Josephson (LMG) Hamiltonian [48, 49]

$$H = \kappa\hat{a}^{\dagger}\hat{b} + \kappa\hat{b}^{\dagger}\hat{a} + \frac{g}{2}[\hat{a}^{\dagger 2}\hat{a}^{2}] + \frac{g}{2}[\hat{b}^{\dagger 2}\hat{b}^{2}] \tag{37}$$

($\hbar = 1$). This Hamiltonian is well described in the literature and models a Bose-Einstein condensate (BEC) constrained to two potential wells of an optical lattice [16, 17, 19, 21–23, 41, 45, 50]. The occupation of each well is modelled as a single mode (boson operators $\hat{a}\dagger, \hat{a}$ and $\hat{b}^{\dagger}, \hat{b}$ respectively). The nonlinearity is quantified by g and the tunnelling between wells by κ. We consider a system prepared with a definite number N of atoms in one mode (well) (that denoted by $\hat{a}$). Since the number of particles is conserved, the state at any later time is of the form (2). The Hamiltonian can be represented in matrix form and the time dependence of the d_m solved as explained in Refs. [16, 21, 22, 50].

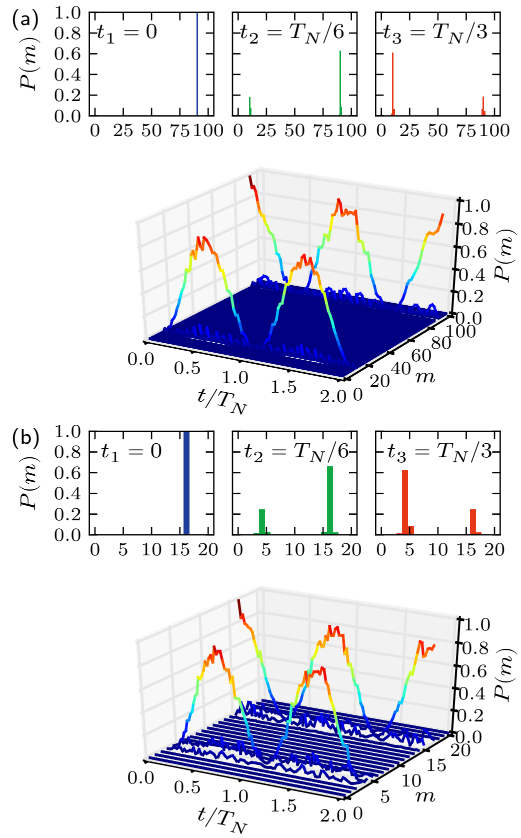

Figure 6: *Mesoscopic two-state oscillation and generation of NOON-type states:* Top: $N = 100$, $g = 2$, $n_L = 10$. Below: $N = 20$, $g = 4$, $n_L = 4$. Time t is in units κ.

B. Two-state oscillation and creation of NOON-states

Solutions give the probability $P(m) = |d_m|^2$ of measuring m particles in the well A at a given time. For some parameters, the population oscillates between wells and there is an almost complete transfer to the well B at some tunnelling time T_N. For larger nonlinearity g, the system can approximate a dynamical two-state system, showing oscillations between the two distinguishable states $|N\rangle|0\rangle$ and $|0\rangle|N\rangle$ over long timescales (Figure 5). At intermediate times ($\sim T_N/2$) before the complete tunnelling from one state to the other, approximate NOON states can be formed. Figure 6 depicts the probabilities $P(m)$ at the intermediate times $T_N/6$ and $T_N/3$ that violate a Leggett-Garg inequality [27, 28]. It is known however that even for moderate N, the predicted tunnelling times T_N are typically much longer than practical decoherence times [19, 21, 51, 52]. For instance, Carr et al report impossibly long times for the typical parameters of Rb atoms [21].

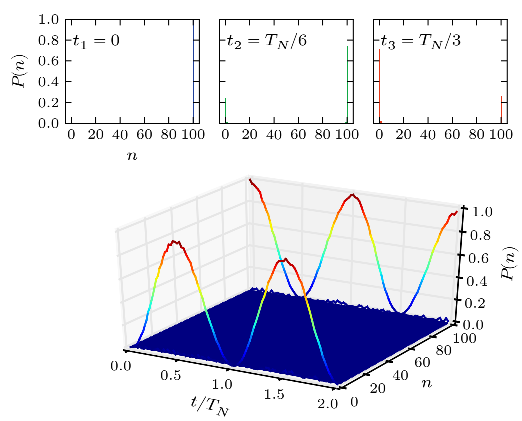

Figure 5: *Two-state mesoscopic dynamics: The creation of NOON states.* Top: Probability $P(m)$ for the number of atoms in well a at times $t_1 = 0$, $t_2 = T_N/6$, $t_3 = T_N/3$. Here $2j_z = 2m - N$. Beneath shows the two-state oscillation. We use $N = 100$, $g = 1$. Time t is in units κ.

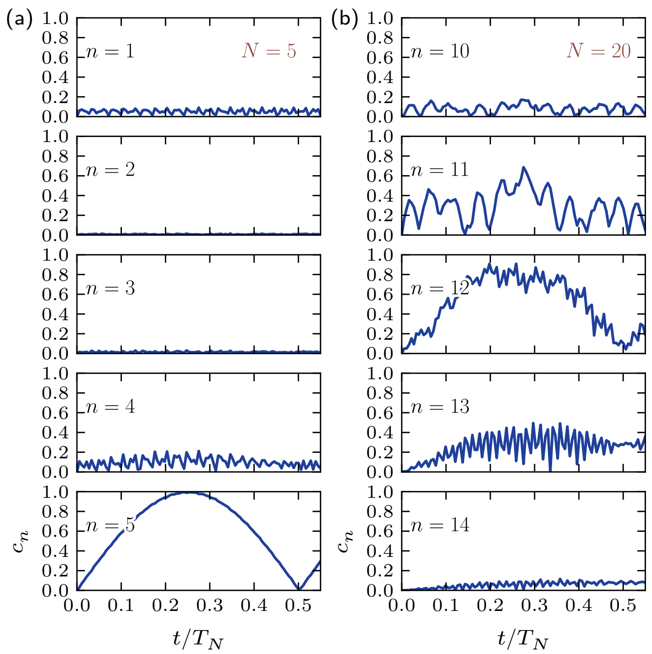

Figure 7: *Signifying the creation of NOON-type states under the Hamiltonian (37):* The n-th order quantum coherence measure c_n versus time t in units κ. Left: $N = 5$, $g = 10$, $n_L = 0$. The NOON state $N = 5$ is signified by $c_5 = 1$, $c_i \sim 0$ ($i \neq 5$) at $t = T_N/4$. Right: $N = 20$, $g = 4$, $n_L = 4$ as for Figure 6b. The large quantum coherence c_n for $n = 12$ signifies the superposition (38) at $t = T_N/4$.

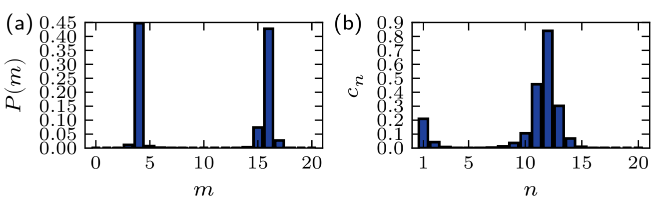

Figure 8: Plot of $P(m)$ and the nth order quantum coherence c_n for the state of Figure 6b at $t = T_N/4$ (as in Figure 7b).

C. Creation of n-scopic quantum superpositions

It is possible however to generate states with a significant mesoscopic coherence by preparing the system in an initial state $|n_L\rangle|N - n_L\rangle$ where $n_L \neq 0, N$. As pointed out by Gordon and Savage [19] and Carr et al [21], the Hamiltonian (37) predicts (in some parameter regimes) an approximate two-state oscillation between the two states $|n_L\rangle|N - n_L\rangle$ and $|N - n_L\rangle|n_L\rangle$. At approximately half the time for oscillation from one state to the other, an n-scopic superposition state of the type given by (12) where $m', n' \neq 0$ is formed i.e.

$$|\psi\rangle = \frac{1}{\sqrt{2}}\{|n_L\rangle|N - n_L\rangle + |N - n_L\rangle|n_L\rangle\} \tag{38}$$

Here, $n = N - 2n_L$. Such n-scopic superposition states have been called "embedded" cat-states [21]. These embedded cat-states are identical to those superpositions (12) discussed in the previous section. Calculations reveal that for some parameters, the period of oscillation reduces to practical values [19, 21]. Two-state oscillation of the BEC has been experimentally observed [26]. We present in Figure 6 predictions for this type of oscillation with $N = 20$ and $n_L = 2$ where the solutions indicate states (38) with a separation of $n = 16$ atoms.

The question becomes how to certify the *quantum coherence* of the embedded cat-states (38) that may be generated in the experiment where such oscillation is observed. The value of the catness-fidelity signature c_n is calculated and given in Figure 7, for the parameters of Figure 6. The c_n for moderate n would feasibly be measurable using higher order interference in multi-atom detection, as described in Section VII.

VII. MEASUREMENT OF MESOSCOPIC QUANTUM COHERENCE VIA $\langle \hat{a}^{\dagger n}\hat{b}^n\rangle$

Finally, we address how one may measure the correlation $\langle \hat{a}^{\dagger n}\hat{b}^n\rangle$. The measurement of J_Z is a photon or atom number difference, achievable with counting detectors or imaging. Schwinger spin operators $J_X = (a^\dagger b + b^\dagger a)/2$, $J_Y = \left(a^\dagger b - b^\dagger a\right)/2i$ are measured similarly as a number difference, after rotating to a different mode pair using polarisers [53]; or Rabi rotations with $\pi/2$ pulses [41, 44, 45]; or beam splitters and phase shifts.

A. Interferometric detection

For instance, we consider the measurable output number difference I_D after transforming the incoming modes a, b to new modes c, d via a 50/ 50 beam splitter and phase shift φ:

$$\begin{aligned} I_D &= \hat{c}^\dagger\hat{c} - \hat{d}^\dagger\hat{d} \\ &= \hat{a}^\dagger\hat{b}e^{i\phi} + \hat{a}\hat{b}^\dagger e^{-i\phi} \\ &= 2J_X\cos\phi - 2J_Y\sin\phi \end{aligned} \tag{39}$$

Here the transformed boson operators for the new modes are $\hat{c} = (\hat{a} + \hat{b}\exp^{i\phi})/\sqrt{2}$, $\hat{d} = (\hat{a} - \hat{b}\exp^{i\phi})/\sqrt{2}$. Selecting $\phi = 0$ or $\phi = -\pi/2$ measures J_X or J_Y. For $N = 1$, $\langle \hat{a}^\dagger\hat{b}\rangle = \langle J_X + iJ_Y\rangle$. The first order moment $\langle \hat{a}^\dagger\hat{b}\rangle$ is thus measurable via the fringe visibility in I_D as one varies ϕ i.e. that $\langle a^\dagger b\rangle$ is nonzero is detectable via first order interference. Similar transformations using atom interferometry give the same results as explained in Ref. [54]. If we have a NOON state incident on the interferometer, the nonzero value of $\langle \hat{a}^{\dagger N}\hat{b}^N\rangle$ can be deduced by observation of higher order interference fringes that are signified by an $e^{iN\phi}$ oscillation. This is the usual method for detecting NOON states [11–13, 22].

The method can also be used to detect and quantify the nth order quantum coherence c_n. We consider that we have a fixed total number N of particles so the input state is of the form (2). The probability of detecting N quanta at the output denoted by mode c is $\langle \hat{c}^{\dagger N}\hat{c}^{N}\rangle/N!$. The probability of obtaining M particles at the port c is a calculable function of the correlation functions $\langle \hat{c}^{\dagger n}\hat{c}^{n}\rangle$ where $n \geq M$. Suppose we measure $\langle \hat{c}^{\dagger n}\hat{c}^{n}\rangle$ for a given fixed n. Expanding we find

$$\begin{aligned}\langle \hat{c}^{\dagger n}\hat{c}^{n}\rangle &= \frac{1}{2^n}\langle(\hat{a}^{\dagger}+\hat{b}^{\dagger}e^{-i\phi})^n(\hat{a}+\hat{b}e^{i\phi})^n\rangle \\ &= \frac{1}{2^n}\sum_{m=0}^{n}\begin{pmatrix} n \\ m\end{pmatrix}\sum_{\ell=0}^{n}\begin{pmatrix} n \\ \ell\end{pmatrix} \\ &\quad \times\langle(\hat{a}^{\dagger})^{n-m}(\hat{b}^{\dagger})^{m}(\hat{a})^{n-\ell}\hat{b}^{\ell}\rangle e^{i\phi(\ell-m)} \quad (40)\end{aligned}$$

The terms that oscillate as $e^{in\phi}$ are proportional to the nth order moment $\langle \hat{a}^{\dagger n}\hat{b}^{n}\rangle$. Hence, if we measure $\langle \hat{c}^{\dagger n}\hat{c}^{n}\rangle$, the fringe visibility associated with this oscillation allows determination of the magnitude of $\langle \hat{a}^{\dagger n}\hat{b}^{n}\rangle$. Where $\langle \hat{a}^{\dagger n}\hat{b}^{n}\rangle$ is the only nonzero moment (as for the ideal NOON states with $n = N$), only the oscillation $e^{in\phi}$ will contribute and the higher order interference enable a clear signature and quantification of the nth order quantum coherence $\langle \hat{a}^{\dagger n}\hat{b}^{n}\rangle$.

For nonideal NOON states the interference method becomes less precise. However, the rapidly oscillating terms can only arise from moments that indicate a higher order of quantum coherence. This is evident by the last line of (40). The moments are of form $\langle(\hat{a}^{\dagger})^{n-m}\hat{a}^{n-\ell}\hat{b}^{\dagger m}\hat{b}^{\ell}\rangle e^{i\varphi(\ell-m)}$ so the oscillation frequency where $l-m=n$ requires $l=n$ and $m=0$ and therefore has a nonzero amplitude only if $\langle \hat{a}^{\dagger n}\hat{b}^{n}\rangle \neq 0$, which is a signature for a quantum coherence of order n. Similarly, the oscillation frequency $l-m=n-1$ requires a nonzero quantum coherence of order $n-1$. While the $\langle \hat{c}^{\dagger n}\hat{c}^{n}\rangle$ can be evaluated from the probabilities for particle counts, in practice for large numbers N, resolution of atom or photon number is difficult. Here one can measure the probability that n is in a binned region the n e.g. the region $n > M$. This probability is given by

$$P(n \geq M) = \sum_{n\geq M}\varsigma\langle \hat{c}^{\dagger n}\hat{c}^{n}\rangle/M!$$

where ς are calculable constants. Here, measurement of a nonzero amplitude for oscillations $e^{iM\phi}$ with frequency M or greater is evidence of quantum coherence of order $\gtrsim M$. The high frequency oscillation can only arise from the high order quantum coherence terms. In Figure 9, we plot $P(n > M)$ and the Fourier analysis for the two-mode example given in Figure 6b.

B. Spin squeezing observables and quadrature phase amplitudes

An alternative method is given in Ref. [54] for $N = 2$. We note that

$$\langle \hat{a}^{\dagger 2}\hat{b}^{2}\rangle = \langle \hat{J}_X^2\rangle - \langle \hat{J}_Y^2\rangle + i\langle\{\hat{J}_X,\hat{J}_Y\}\rangle \quad (41)$$

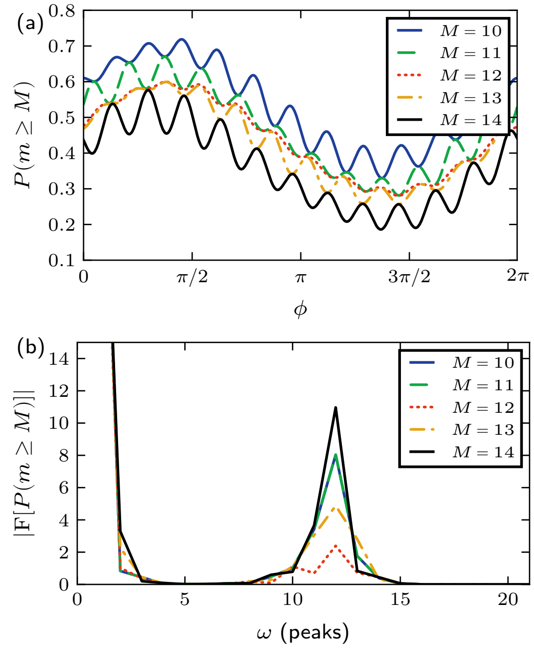

Figure 9: (a) The probability of measuring more or equal to M photons, for $N = 20$, $g = 4$, $n_L = 4$ at $t = T_N/4$ (same as in Fig. 7b) after a rotation. (b) The Fourier transform of the curves from (a), plotted against angular frequency (which is equivalent to the number of oscillations in the range of 2π), showing a significant peak at $\omega = 12$ (the expected separation of the state, $(|4\rangle|16\rangle + |16\rangle|4\rangle)/\sqrt{2})$ for all M.

where $\{A, B\} \equiv AB + BA$. The real part of $\langle \hat{a}^{\dagger 2}\hat{b}^{2}\rangle$ can be evaluated by measurement of $\langle \hat{J}_X^2\rangle$ and $\langle \hat{J}_Y^2\rangle$. We show that the moment is nonzero if we can show that $\langle \hat{J}_X^2\rangle \neq \langle \hat{J}_Y^2\rangle$. If necessary, the imaginary part can be determined by measurement of suitably rotated spin observables defined by $\hat{J}_\theta = \hat{J}_X\cos\theta - \hat{J}_Y\sin\theta$.

For $N = 3$ manipulation gives (see Appendix for details)

$$\begin{aligned}\left\langle \hat{a}^{\dagger 3}\hat{b}^{3}\right\rangle &= 2\left\langle \hat{J}_X^3\right\rangle - \sqrt{2}(\langle \hat{J}^3_{\frac{\pi}{4}}\rangle + \langle \hat{J}^3_{\frac{3\pi}{4}}\rangle) \\ &\quad -2i\left\langle \hat{J}_Y^3\right\rangle + i\sqrt{2}(\langle \hat{J}^3_{\frac{\pi}{4}}\rangle + \langle \hat{J}^3_{\frac{3\pi}{4}}\rangle) \quad (42)\end{aligned}$$

where $\langle \hat{J}_\theta^3\rangle$ are measurable by standard interferometry/ atom interferometry techniques.

We note that similar expansions can be made expressing the a and b operators in terms of quadrature phase amplitudes X and P. For optical NOON states, this may be a useful way to accurately measure the moments $\langle \hat{a}^{\dagger M}\hat{b}^{M}\rangle$ since quadrature phase amplitudes can be measured with high efficiency. Specifically, we define the amplitudes $\hat{X}$ and $\hat{P}$ by $\hat{a} = \hat{X}_A + i\hat{P}_A$ and $\hat{b} = \hat{X}_B + i\hat{P}_B$. Hence (we drop the "hats" for convenience)

$$\langle \hat{a}^{\dagger}\hat{b}\rangle = \langle \hat{X}_A\hat{X}_B\rangle + \langle \hat{P}_A\hat{P}_B\rangle - i\langle \hat{P}_A\hat{X}_B + \hat{X}_A\hat{P}_B\rangle \quad (43)$$

which is readily measurable. Continuing

$$\begin{aligned}\langle \hat{a}^{\dagger 2}\hat{b}^2\rangle &= \langle(\hat{X}_A^2-\hat{P}_A^2)(\hat{X}_B^2-\hat{P}_B^2)\rangle+\langle\{\hat{X}_A,\hat{P}_A\}\{\hat{X}_B,\hat{P}_B\}\rangle\\ &\quad -i\langle\{\hat{X}_A,\hat{P}_A\}(\hat{X}_B^2-\hat{P}_B^2)\rangle\\ &\quad +i\langle(\hat{X}_A^2-\hat{P}_A^2)\{\hat{X}_B,\hat{P}_B\}\rangle \end{aligned} \quad (44)$$

The anticommutator is measurable by rotation of the quadratures. We define the measurable rotated quadrature phase amplitudes as $\hat{X}_\theta=\hat{X}\cos(\theta)+\hat{P}\sin(\theta)$ and $\hat{P}_\theta=-\hat{X}\sin(\theta)+\hat{P}\cos(\theta)$. Hence, $\hat{X}_{\pi/4}=\frac{1}{\sqrt{2}}\{\hat{X}+\hat{P}\}$ and $\hat{P}_{\pi/4}=\frac{1}{\sqrt{2}}\{-\hat{X}+\hat{P}\}$ and we note that $\langle\hat{X}_{\pi/4}^2\rangle=\langle\hat{X}^2+\hat{P}^2+\hat{X}\hat{P}+\hat{P}\hat{X}\rangle/2$. Thus, we can deduce either $\{\hat{X},\hat{P}\}$ by measuring the moments $\langle\hat{X}^2\rangle$, $\langle\hat{P}^2\rangle$ and $\langle\hat{X}_{\pi/4}^2\rangle$.

C. Experimental certification of atomic quantum coherence $n\sim 2$ by inferring the correlation $\langle\hat{a}^{\dagger n}\hat{b}^n\rangle$ from spin squeezing

Esteve et al. experimentally realise the system modelled by the two-mode Hamiltonian [41]. The ground state solutions have been solved and studied in Ref [23]. Esteve et al report data obtained on cooling their two-well system, including measurements for the spin moments $\langle\hat{J}_\theta^2\rangle$ associated with ultra-cold atomic mode populations of two wells of the optical lattice [41]. Their observations analyse the variances of the Heisenberg uncertainty principle

$$\Delta\hat{J}_z\Delta\hat{J}_y\geq|\langle\hat{J}_x\rangle|/2\sim N/4 \quad (45)$$

They report spin squeezing in $\hat{J}_z$ with enhanced noise in $\hat{J}_y$. They also report $\langle\hat{J}_z\rangle\sim 0$ and $\langle\hat{J}_y\rangle\sim 0$. Hence we can conclude

$$\langle\hat{J}_z^2\rangle<N/4<\langle\hat{J}_y^2\rangle \quad (46)$$

Thus we deduce

$$\langle\hat{J}_y^2\rangle-\langle\hat{J}_z^2\rangle\neq 0 \quad (47)$$

which implies $\langle\{\hat{J}_{cx},\hat{J}_{cy}\}\rangle\neq 0$ where $\hat{J}_{cx}$, $\hat{J}_{cy}$ are Schwinger operators defined for the rotated modes $\hat{c}=(\hat{a}+\hat{b})/\sqrt{2}$ and $\hat{d}=\frac{e^{-i\pi/4}}{\sqrt{2}}(\hat{a}-\hat{b})$. Hence we conclude

$$|\langle\hat{c}^{\dagger 2}\hat{d}^2\rangle|\neq 0 \quad (48)$$

which (using the Results of Section III) gives evidence in their BEC system of a two-atom coherence i.e. a generalised n-scopic superpositions with $n=2$ of type

$$|\psi_2\rangle=c_{20}|2\rangle_c|0\rangle_d+c_{11}|1\rangle_c|1\rangle_d+c_{02}|0\rangle_c|2\rangle_d+\psi_0 \quad (49)$$

where the coefficients satisfy $c_{02}\neq 0$ and $c_{20}\neq 0$ and where ψ_0 is orthogonal to each of $|2\rangle_c|0\rangle_d$, $|1\rangle_c|1\rangle_d$ and $|0\rangle_c|2\rangle_d$. We note that this is consistent with the predictions of [23] for the nonzero moments $\langle\hat{c}^{\dagger 2}\hat{d}^2\rangle\neq 0$ for the populations of modes c,d in atomic systems with $\kappa<0$. The observation of $\langle\hat{a}^{\dagger 2}\hat{b}^2\rangle\neq 0$ would be evidence of a superposition of atoms constrained to the modes of the wells

$$|\psi_2\rangle=c_{20}|2\rangle_a|0\rangle_b+c_{11}|1\rangle_a|1\rangle_b+c_{02}|0\rangle_a|2\rangle_b+\psi_0 \quad (50)$$

where $c_{02}\neq 0$ and $c_{20}\neq 0$. This is predicted for atomic BEC with $\kappa>0$ [23]. Three-atom superpositions (for which $\langle\hat{a}^{\dagger 3}\hat{b}^3\rangle\neq 0$) and higher are also predicted (up to N) and should be evident via higher order fringe patterns, or else directly via the J_θ measurements as above.

D. Entanglement

The observation of the nth order quantum coherence $\langle\hat{a}^{\dagger n}\hat{b}^n\rangle\neq 0$ is not in itself sufficient to imply entanglement. For instance ψ_0 in the expression (49) might include contributions from terms such as $|2\rangle|2\rangle$ and $|0\rangle|0\rangle$. This means that a separable form for $|\psi\rangle$ e.g.

$$|\psi\rangle=\frac{1}{2}(|2\rangle_c+|0\rangle_c)(|2\rangle_d+|0\rangle_d)$$

may be possible. The separable state contrasts with the "dead here-alive there" entangled superposition state whose ideal form is precisely the NOON state e.g. for $N=2$

$$|\psi_2\rangle=\frac{1}{\sqrt{2}}\{|2\rangle_c|0\rangle_d+|0\rangle_c|2\rangle_d\}$$

In this paper, we are only concerned with how to certify an n-scopic quantum superposition, without regard to entanglement. However, the entangled case is of special interest, especially where the two modes are spatially separated. For the ideal NOON case, we therefore point out that one can make simple measurements to confirm the entanglement. If one measures the individual mode numbers n_a and n_b, the results 0 or N are obtained for each mode. The observations would be correlated, so that there is *only* a nonzero probability to obtain $|N\rangle|0\rangle$ or $|0\rangle|N\rangle$. This eliminates the possibility of nonzero contributions from terms in ψ_0 and it remains only to confirm the nonzero quantum coherence in order to confirm the entanglement. The observation of $\langle\hat{a}^{\dagger N}\hat{b}^N\rangle\neq 0$ then becomes sufficient to certify the entanglement of the NOON state. While simple in principle, this procedure is not so useful in practice. For example, the attenuated NOON state of Section V would predict a nonzero probability for obtaining $|0\rangle|0\rangle$ and a more careful analysis is necessary to deduce entanglement.

VIII. CONCLUSION

We have examined how to rigorously confirm and quantify the mesoscopic quantum coherence of non-ideal

NOON states. In this paper, we link the observation of quantum coherence to the negation of certain types of mixtures, given as (3) and (4). However it is stressed we are restricting to mixtures where the "dead" and "alive" states are *quantum* states that can therefore be represented by density operators (ρ_A and ρ_D in the equation (3)). This contrasts with other possible signatures of a cat-state where the dead and alive states might also be hidden variable states, as in Ref. [27].

In this paper, we have focused on two criteria for the *n-th order quantum coherence*, defined as a quantum coherence between number states different by n quanta. The first criterion is a nonzero nth order moment $\langle \hat{a}^{\dagger n}\hat{b}^{n}\rangle \neq 0$ and the second is a quantifiable amount of Schwinger spin squeezing. We have shown how the first criterion can be a *quantifier* of the overall nth order coherence. The second criterion can be a robust and effective signature for large n, and can verify high orders of coherence in existing atomic experiments, but does not signify all cases of n-scopic quantum coherence. In Sections V-VI, we have illustrated the use of the criteria with the examples of attenuated NOON states, number states $|N\rangle$ that pass through beam spitters, and approximate NOON states formed from N particles via nonlinear interactions. These examples model recent photonic and atomic BEC experiments.

In Section VII, we have examined how the moments $\langle \hat{a}^{\dagger n}\hat{b}^{n}\rangle$ might be measured. Optical NOON states are normally verified by nth order interference fringes, which imply $\langle \hat{a}^{\dagger n}\hat{b}^{n}\rangle \neq 0$. Direct photon detection normally introduces high losses which creates low fidelities that may make significant statistics difficult, except with post selection. We suggest that to obtain higher cat-fidelities the moments can be measured via high efficiency quadrature phase amplitude detection.

Finally, in Section VIII, we analyse data from experiments, noting that the signatures do not directly prove entanglement i.e. do not distinguish between a local superpositions of type $|N\rangle + |0\rangle$ for one mode, and the entangled superposition of the NOON state. Hence we cannot conclude a superposition of states with different mass locations, although we believe this could be possible using for instance the entanglement criteria presented in Refs. [22, 54, 55].

Acknowledgements

We thank P. Drummond, B. Dalton, Q. He and those at the 2016 Heraeus Seminar on Macroscopic Entanglement for discussions on topics related to this paper. We are grateful to the Australian Research Council for support through its Discovery Projects program.

Appendix A: Result 2

To explain the connection between the condition $\langle \hat{a}^{\dagger n}\hat{b}^{n}\rangle \neq 0$ and the superposition state (12) in detail, consider the most general two-mode quantum state for this two-mode system that cannot be a superposition of two states distinct by n quanta. We note that any pure state $|\psi_{ent}\rangle$ can be expanded in the two-mode number (Fock) state basis:

$$\begin{aligned}|\psi_{ent}\rangle &= \sum_{n,m} c_{nm}|n_a\rangle|m_b\rangle \\ &= c_{00}|0\rangle|0\rangle + c_{01}|0\rangle|1\rangle + c_{10}|1\rangle|0\rangle \\ &\quad + c_{11}|1\rangle|1\rangle + c_{12}|1\rangle|2\rangle + c_{21}|2\rangle|1\rangle \\ &\quad + c_{02}|0\rangle|2\rangle + c_{20}|2\rangle|0\rangle + ...\end{aligned}$$

We see that if $\langle \hat{a}^{\dagger n}\hat{b}^{n}\rangle \neq 0$, then the state is necessarily of the form (12)which involves a superposition of two states distinct by n quanta. We note that when $\langle \hat{a}^{\dagger n}\hat{b}^{n}\rangle \neq 0$, the density operator ρ for the system cannot be written in an alternative form except to provide a nonzero coherence (10) between states $|n'\rangle|m'+n\rangle$ and $|n'+n\rangle|m'\rangle$. We conclude that the diagonal elements ${}_b\langle m'+n|_a\langle n'|\rho|n'\rangle_a|m'+n\rangle_b$ and ${}_b\langle m'|_a\langle n'+n|\rho|n'+n\rangle_a|m'\rangle_b$ are also nonzero. Thus, there is a nonzero probability P_D that the system is found in state $|n'\rangle|m'+n\rangle$ (that we call "dead") and also a nonzero probability P_A that the system is found in state $|n'+n\rangle|m'\rangle$ (that we call "alive"). Yet, the superposition state (12) cannot be given as a classical mixture (9) which has a zero coherence between the states $|n'\rangle|m'+n\rangle$ and $|n'+n\rangle|m'\rangle$ whose $2J_z$ values are different by n.

Appendix B: Proof of Result 3 for Spin squeezing test

We follow from the main text and generalise to consider a two-mode description of the state as given by for a mixed state by a density operator ρ. We expand in terms of pure states $|\psi_R\rangle$ so that $\rho = \sum_R P_R|\psi_R\rangle\langle\psi_R|$ for some probabilities P_R. Each pure state $|\psi_R\rangle$ can be expressed as a superposition of number eigenstates given by (14). We know that the variance $(\Delta\hat{J}_Y)^2$ of any mixture satisfies $(\Delta\hat{J}_Y)^2 \geq \sum_R P_R(\Delta\hat{J}_Y)^2_R$. Thus

$$(\Delta\hat{J}_Y)^2 \geq \sum_R P_R(\Delta\hat{J}_Y)^2_R \geq \sum_R P_R\frac{|\langle\hat{J}_X\rangle_R|^2}{4(\Delta\hat{J}_Z)^2_R}$$

For all the possible mixtures denoted by a choice of set $\{|\psi_R\rangle\}$ (where $P_R \neq 0$) we can determine the spread δ_R for each state $|\psi_R\rangle$ and then select the maximum of the set δ_R and call it δ_0. We select the mixture set consistent with the density operator that has the minimum possible value of δ_0: That is, we determine that the density operator cannot be expanded in a set $|\psi_R\rangle$ with a smaller δ_0. Then for the pure states of this set $|\psi_R\rangle$, the maximum variance in $\hat{J}_Z$ is $(\Delta\hat{J}_Z)^2 = \delta_0^2/4$ i.e. $(\Delta\hat{J}_Z)^2_R \leq \delta_0^2/4$.

Then we see that the uncertainty relation (16) implies a minimum value for the variance in $\hat{J}_Y$:

$$(\Delta\hat{J}_Y)_R^2 \;\geq \tfrac{|\langle\hat{J}_X\rangle_R|^2}{4(\Delta J_Z)_R^2} \;\geq \frac{1}{\delta_0^2}|\langle\hat{J}_X\rangle_R|^2$$

Simplification gives

$$\begin{aligned}(\Delta\hat{J}_Y)^2 \;&\geq\; \frac{1}{\delta_0^2}\sum_R P_R|\langle\hat{J}_X\rangle_R|^2 \geq \frac{1}{\delta_0^2}|\sum_R P_R\langle\hat{J}_X\rangle_R|^2\\ &=\; \frac{1}{\delta_0^2}|\langle\hat{J}_X\rangle|^2\end{aligned}$$

Taking the case of the spin squeezing experiments where measurements give $\langle\hat{J}_X\rangle \sim \langle N\rangle/2$, we see that

$$(\Delta\hat{J}_Y)^2 \geq \frac{1}{\delta_0^2}|\langle\hat{J}_X\rangle|^2 = \frac{\langle N\rangle^2}{4\delta_0^2} \tag{B1}$$

Thus there is a lower bound on the best amount of squeezing determined by the maximum spread (extent) δ_0 of the superposition. We can now prove the Result 3: The measured amount of squeezing places a lower bound on the extent δ_0 of the broadest superposition: Thus if the measured squeezing is ξ_N, then from (B1) the underlying state has a minimum breadth δ_0 of superposition (in the eigenstates of $\hat{J}_Z$) given by $\delta_0 > \frac{\langle N\rangle}{2(\Delta J_Y)} = \frac{\sqrt{N}}{\xi_N}$. The width δ_0 of the superposition gives the extent or size of the coherence i.e. the value of n in the expression (12).

Appendix C: Catness-fidelity quantifier for mixed states

Discussion in terms of superposition states: We give the proof of Result (4) in terms of the superposition states. The experiment may confirm a range of values of j_z for J_z for which $\langle\hat{a}^{\dagger 2j_z}\hat{b}^{2j_z}\rangle \neq 0$. Take one such value: $2j_z = N_0$. Then we know there is a nonzero probability P_{N_0} that the system be in a superposition of form

$$\begin{aligned}|\psi_{N_0}\rangle_{nm} \;&=\; a_{N_0}^{(n,m)}|n\rangle|m+N_0\rangle + b_{N_0}^{(n,m)}|n+N_0\rangle|m\rangle\\ &\quad +c|\psi\rangle\end{aligned} \tag{C1}$$

where $a_{N_0}^{(n,m)}$,$b_{N_0}^{(n,m)} \neq 0$. Based on the measured moments, we can write the density operator in the general form

$$\rho = \sum_{n,m} P_{N_0}^{(n,m)}\rho_{N_0}^{(n,m)} + P_{mix}\rho_{mix} + P_n\rho_n \tag{C2}$$

where $\rho_{N_0} = |\psi_{N_0}\rangle\langle\psi_{N_0}|$, ρ_{mix} is a mixture of states $|n\rangle|m+N_0\rangle$ and $|n+N_0\rangle|m\rangle$, and ρ_n is a state that gives predictions different to $j_z = \pm N_0/2$. Only the first term will contribute a nonzero value of $\langle a^{\dagger N_0}b^{N_0}\rangle$. The first term can also include superpositions of the different $|\psi_{N_0}\rangle$ with different n, m but evaluation of the moment $\langle a^{\dagger N_0}b^{N_0}\rangle$ will be the same as if the system were in a mixture of those states (due to the orthogonality). The *relevant* (Re) values of n, m such that probabilities are nonzero can be determined from the measurements of mode number and we assume the sums only includes those nonzero contributions. We note that the first term is written as a mixture of the NOON-type states. In some cases, such a mixture can be equivalent to (and therefore rewritten as) a classical mixture ρ_{mix}, but the nonzero moment $\langle\hat{a}^{\dagger N}\hat{b}^N\rangle$ cannot arise in this case. The value of $\langle\hat{a}^{\dagger N}\hat{b}^N\rangle$ is zero for any ρ_{mix}, and the prediction for $\langle\hat{a}^{\dagger N}\hat{b}^N\rangle$ given by ρ is

$$\begin{aligned}|\langle\hat{a}^{\dagger N_0}\hat{b}^{N_0}\rangle| \;&=\; |\sum_{n,m} a_{N_0}^{(n.m)}b_{N_0}^{(n,m)*}P_{N_0}^{(n,m)}\\ &\qquad\times\sqrt{\frac{(m+N_0)!}{m!}}\sqrt{\frac{(n+N_0)!}{n!}}|\\ &\leq\; S\sum_{n,m}|a_{N_0}^{(n,m)}b_{N_0}^{(n,m)*}P_{N_0}^{(n,m)}|\end{aligned} \tag{C3}$$

We have used the prediction for $\langle a^{\dagger N_0}b^{N_0}\rangle$ for the state $|\psi_{N_0}\rangle$ and the definitions of S as in the main text. The measurement of the moment $\langle\hat{a}^{\dagger N_0}\hat{b}^{N_0}\rangle$ thus allows the determination of a lower bound on an effective fidelity for the Schrodinger cat NOON state.

Correction term: Now we consider that the experimentalist can only confirm that the total probability of the "nonrelevant" (NRe) outcomes is less than or equal to ϵ. The contribution of the "nonrelevant" terms to the C_{N_0} (the sum of the N_0-th order coherences) is bounded by the probabilities. For any density matrix, the off-diagonal elements are bounded by the diagonal elements that give the probabilities: Always $a_{N_0}^{(n.m)}b_{N_0}^{(n,m)*} \leq \frac{1}{2}$ and assuming $\sum_{NRe} P_{N_0}^{(n,m)} \leq \epsilon$, we find

$$\sum_{NRe} a_{N_0}^{(n.m)}b_{N_0}^{(n,m)*}P_{N_0}^{(n,m)} \leq \epsilon/2$$

Using that $\frac{(n+N_0)!}{n!} \leq (n+N_0)^{N_0}$, this implies

$$\begin{aligned}\langle\hat{a}^{\dagger N_0}\hat{b}^{N_0}\rangle \;&\leq\; \sum_{Re} a_{N_0}^{(n.m)}b_{N_0}^{(n,m)*}P_{N_0}^{(n,m)}\\ &\qquad\times\sqrt{\frac{(m+N_0)!}{m!}}\sqrt{\frac{(n+N_0)!}{n!}}\\ &\qquad+\sum_{NRe} a_{N_0}^{(n.m)}b_{N_0}^{(n,m)*}P_{N_0}^{(n,m)}(N_{up}+N_0)^{N_0}\\ &\leq\; S\sum_{n,m}|a_{N_0}^{(n,m)}b_{N_0}^{(n,m)*}P_{N_0}^{(n,m)}| + \frac{\epsilon}{2}(N_{up}+N_0)^{N_0}\end{aligned} \tag{C4}$$

Thus we know that

$$\begin{aligned}C_{N_0} \;&\geq\; \sum_{Re} a_{N_0}^{(n.m)}b_{N_0}^{(n,m)*}P_{N_0}^{(n,m)}\\ &\geq\; [\langle\hat{a}^{\dagger N_0}\hat{b}^{N_0}\rangle - \frac{\epsilon}{2}(N_{up}+N_0)^{N_0}]/S\end{aligned} \tag{C5}$$

where N_{up} is the upper bound for the mode numbers, given that the system cannot have infinite mode or particle (atom) number. For the cases of interest to us on this paper, the total mode number is the atom number N, which is fixed.

Appendix D: Evaluation of Normalisation

We consider the state

$$|out\rangle = \sum_{m=0}^{N} d_m |m\rangle_a |N-m\rangle_b \,, \tag{D1}$$

We quantify the n-th order quantum coherence by the parameter C_n (that we have also called the catness-fidelity)

$$C_n = \mathcal{N}_{n,N} \sum_{m=0}^{N-n} |d_m d^*_{m+n}| \tag{D2}$$

where $\mathcal{N}_{n,N}$ is a normalisation constant to ensure the maximum value of C_n is 1. The normalisation $\mathcal{N}_{n,N}$ is determined by the bounds on the coherences of the density matrix for a pure state. For example, where $n = N$, the maximum $|d_0 d^*_N|$ is obtained for $d_0 = d_N = \frac{1}{\sqrt{2}}$ with all other amplitudes zero. Hence $|d_0 d^*_N| \le 1/2$ and $\mathcal{N}_{N,N} = 2$. Similarly, for $n = N-1$ and $N \ge 3$ (so that the d terms in $d_0 d^*_{N-1} + d_1 d^*_N$ are all different), we find $d_0 d^*_{N-1} + d_1 d^*_N \le 1/2$ where in this case the maximum $\sum_{m=0}^{N-n} |d_m d^*_{m+n}|$ is found taking $d_0 = d_{N-1} = d_1 = d_N = \frac{1}{2}$. The maximum value for more general n and N can be found numerically.

(1) We start by analyzing $n = N$. Then $C_n = \mathcal{N}_{n,N} |d_0 d^*_N|$. There is only one term in the sum and therefore only two amplitudes contributing to the sum. The number of terms is independent of N. We can show that the maximum value of the sum of the coherences (namely $\sum_{m=0}^{N-n} |d_m d^*_{m+n}|$) is given when $d_0 = d_N = \frac{1}{\sqrt{2}}$, and all other amplitudes zeros. Hence $C_n \le \mathcal{N}_{n,N} |d_0 d^*_N| = \mathcal{N}_{n,N} \frac{1}{2}$ and the optimal normalisation is $\mathcal{N}_{n,N} = 2$.

(2) Next we consider $n > N/2$. Here $\sum_{m=0}^{N-n} |d_m d^*_{m+n}| = d_0 d_n + d_1 d_{n+1} + ..d_{N-n} d_N$ and since $n > N-n$ the terms in the summation involve different d_i's which can be therefore be chosen independently apart from normalisation requirements. Taking the $2(N-n+1)$ contributing amplitudes as equal, and all other as zero, $\sum_{m=0}^{N-n} |d_m d^*_{m+n}| = \frac{(N-n+1)}{2(N-n+1)} = \frac{1}{2}$ which we verify is the maximum value.

(3) For the remaining values, we determine the bounds numerically. We analyse all these cases and fit an expression for the maximum value of $\sum_{m=0}^{\frac{N}{2}} |d_m d^*_{m+\frac{N}{2}}|$. On numerically analysing the cases $n < N/2$, we find that to a good approximation $\sum_{m=0}^{N-n} |d_m d^*_{m+n}| \le \cos\left(\frac{\pi}{[N/n]+2}\right)$, where $[N/n]$ denotes the integer part of N/n and hence $\mathcal{N}_{n,N} = 1/\cos\left(\frac{\pi}{[N/n]+2}\right)$. We numerically verified this bound for all N up to 500.

Appendix E: Evaluation of $\langle \left(\hat{a}^\dagger \hat{b}\right)^3 \rangle$

For $N = 3$, we would like to measure the expectation value of the following observable

$$\begin{aligned}
\left(\hat{a}^\dagger \hat{b}\right)^3 &= (J_x + iJ_y)^3 \\
&= J_x^3 - iJ_y^3 + i\left(J_x J_y J_x + J_y J_x^2 + J_x^2 J_y\right) \\
&\quad - \left(J_y^2 J_x + J_x J_y^2 + J_y J_x J_y\right).
\end{aligned}$$

In the expansion, we have dropped the "hats" and used lower case x and y in the subscripts of the $\hat{J}_X$ and $\hat{J}_Y$ defined in (13) to simplify notation. The first and second terms can be measured in experiments. However, we need to express $J_x J_y J_x + J_y J_x^2 + J_x^2 J_y$ and $J_y^2 J_x + J_x J_y^2 + J_y J_x J_y$ in terms of some other measurements that can be carried out in experiments. To this end, we define a rotated Schwinger operators as follows:

$$\begin{aligned}
J_\theta &= J_x \cos\theta + J_y \sin\theta \\
J_{\theta+\frac{\pi}{2}} &\equiv G_\theta \\
&= J_x \cos\left(\theta + \frac{\pi}{2}\right) + J_y \sin\left(\theta + \frac{\pi}{2}\right) \\
&= -J_x \sin\theta + J_y \cos\theta.
\end{aligned}$$

For $\theta = \frac{\pi}{4}$, these rotated operators correspond to:

$$\begin{aligned}
J^3_{\frac{\pi}{4}} &= \frac{1}{\sqrt{2^3}} \left[\left(J_y^2 J_x + J_x J_y^2 + J_y J_x J_y\right)\right. \\
&\quad \left. + \left(J_x J_y J_x + J_y J_x^2 + J_x^2 J_y\right) + J_x^3 + J_y^3\right] \\
G^3_{\frac{\pi}{4}} &= \frac{1}{\sqrt{2^3}} \left[-\left(J_y^2 J_x + J_x J_y^2 + J_y J_x J_y\right)\right. \\
&\quad \left. + \left(J_x J_y J_x + J_y J_x^2 + J_x^2 J_y\right) - J_x^3 + J_y^3\right].
\end{aligned}$$

Thus after manipulation we obtain

$$J_y^2 J_x + J_x J_y^2 + J_y J_x J_y = \sqrt{2}\left(J^3_{\frac{\pi}{4}} - G^3_{\frac{\pi}{4}}\right) - J_x^3$$

$$J_x J_y J_x + J_y J_x^2 + J_x^2 J_y = \sqrt{2}\left(J^3_{\frac{\pi}{4}} + G^3_{\frac{\pi}{4}}\right) - J_y^3$$

Using the above expressions, we can then rewrite the moment $\left(a^\dagger b\right)^3$ in terms of the rotated Schwinger operators as:

$$\begin{aligned}\left(\hat{a}^{\dagger}\hat{b}\right)^{3} &= J_x^3 - iJ_y^3 + i\left(J_xJ_yJ_x + J_yJ_x^2 + J_x^2J_y\right)\\ &\quad - \left(J_y^2J_x + J_xJ_y^2 + J_yJ_xJ_y\right)\\ &= J_x^3 - iJ_y^3 + i\left[\sqrt{2}\left(J_{\frac{\pi}{4}}^3 + G_{\frac{\pi}{4}}^3\right) - J_y^3\right]\\ &\quad - \left[\sqrt{2}\left(J_{\frac{\pi}{4}}^3 - G_{\frac{\pi}{4}}^3\right) - J_x^3\right]\\ &= 2J_x^3 - 2iJ_y^3 + \sqrt{2}i\left(J_{\frac{\pi}{4}}^3 + G_{\frac{\pi}{4}}^3\right)\\ &\quad -\sqrt{2}\left(J_{\frac{\pi}{4}}^3 - G_{\frac{\pi}{4}}^3\right).\end{aligned}$$

which leads to the required result.

[1] E. Schroedinger, Naturwiss. **23**, 807 (1935).

[2] A. O. Caldeira and A. J. Leggett, Phys. Rev. A **31**, 1059 (1985). D. F. Walls and G. J. Milburn, Phys. Rev. A **31**, 2403 (1985).

[3] B. Yurke and D. Stoler, Phys. Rev. Lett. **57**, 13 (1986).

[4] M. Brune et al., Phys. Rev. Lett. **77**, 4887 (1996). C. Monroe et al., Science **272**, 1131 (1996). J. Friedman et al., Nature **406** 43 (2000). D. Leibfried et al., Nature **438**, 04251 (2005). A. Ourjoumtsev et al., Nature **448**, 784 (2007). T. Monz et al., Phys. Rev. Lett. **106**, 130506 (2011).

[5] W. Marshall, C. Simon, R. Penrose and D. Bouwmeester, Phys. Rev. Lett., **91**, 130401 (2003). M. Vanner, Phys. Rev. X 1, 021011 (2011). M. R. Vanner et al., Proc. Nat. Ac. Sc. **108**, 16182 (2011). M. Vanner, Phys. Rev. **X** 1, 021011 (2011). I. Pikovski et al., Nat. Phys. **8**, 393 (2012).

[6] G. C. Ghirardi, A. Rimini, and T. Weber, Phys. Rev. D 34, 470 (1986); G. Ghirardi, R. Grassi, A. Rimini, Phys. Rev. A 42, 1057 (1990).

[7] L. Diósi, Phys. Lett. A **120**, 377 (1987); Phys. Rev. A **40**, 1165 (1989); Braz. J. Phys. 35, 260 (2005); J. Phys. A, Math. Theor. **40**, 2989 (2007).

[8] R. Penrose, Gen. Relativ. Gravit. **28**, 581 (1996); Phil. Trans. R. Soc. Lond. A **356**, 1927 (1998); *Mathematical Physics*, pp. 266–282. Imperial College, London (2000).

[9] C. K. Hong, Z. Y. Ou, and L. Mandel, Phys. Rev. Lett. **59**, 2044 (1987). Z. Y. Ou et al., Phys. Rev. A **42**, 2957 (1990). J. Rarity, Phys. Rev. Lett. **65**, 1348 (1990). Phys. Rev. A **42**, 2957 (1990). E. Fonseca, C. Monken and S. Padua, Phys. Rev. Lett. **82**, 2868 (1999). K. Edamatsu, R. Shimizu and T. Itoh, Phys. Rev. Lett. **89**, 213601 (2002).

[10] M. Stobinska et al, Phys. Rev. A **86** 063823 (2012). T. Sh. Iskhakov, K. Yu Spasibko, M. V. Chekhova and G. Leuchs New J. Phys. **15**, 093036 (2013); K. Yu. Spasibko, F. Töppel, T. Sh. Iskhakov, M. Stobińska, M. V. Chekhova, and G. Leuchs, New J. Phys. **16**, 013025 (2014).

[11] J. P. Dowling, Contemporary Physics **49**, 125 (2008). H. Lee, P. Kok and J. P. Dowling, Journal of Modern Optics **49**, 2325 (2002); P. Kok, H. Lee, and J. P. Dowling, Phys. Rev. A **65**, 052104. J. Fiurášek, Phys. Rev. A **65**, 053818 (2002).

[12] P. Walther et al., Nature **429**, 158 (2004). M. W. Mitchell, J. S. Lundeen and A. M. Steinberg, Nature **429**, 161 (2004). Y. Israel et al., Phys. Rev. A **85**, 022115 (2012); H. Kim, H. S. Park, S.-K. Choi, Opt. Express **17**, 19720 (2009). R. Kruse et al., Phys. Rev. A **92**, 053841 (2015).

[13] I. Afek, O. Ambar, Y. Silberberg, Science **328**, 879 (2010).

[14] A. Boto et al., Phys. Rev. Lett. **85**, 2733 (2000). Y.-H. Kim and Y. H. Shih, Found. Phys. **29**, 1849 (1999). M. Angelo, M. Chekhova and Y. Shih, Phys. Rev. Lett. **87**, 13602 (2001). R. W. Boyd and J. P. Dowling, Quantum Information Processing **11**, 891 (2012).

[15] R. J. Lewis-Swan and K. V. Kheruntsyan, Nature Communications **5**, 3752 (2014); S. S. Hodgman et al., Science, **331** (6020), 1046 (2011).

[16] G. J. Milburn et al., Phys. Rev. A **55**, 4318 (1997).

[17] J. I. Cirac et al., Phys. Rev. A **57**, 1208 (1998).

[18] Y. Zhou, H. Zhai, R. Lü, Z. Xu, and L. Chang, Phys. Rev. A **67**, 043606 (2003).

[19] D. Gordon and C. M. Savage, Phys. Rev. A **59**, 4623, (1999). J. Dunningham and K. Burnett, Journ. Modern Optics, **48**, 1837, (2001). C. Lee, Phys. Rev. Lett. **97**, 150402 (2006).

[20] D. R. Dounas-Frazer, A. M. Hermundstad and L. D. Carr, Phys. Rev. Lett. **99**, 200402 (2007).

[21] L. D. Carr, D. R. Dounas-Frazer and M. A. Garcia-March, Europhys. Lett. **90,** 10005 (2010).

[22] T. J. Haigh, A. J. Ferris, and M. K Olsen, Opt. Commun. **283**, 3540 (2010).

[23] Q. Y. He et al., Phys. Rev. A **86**, 023626 (2012).

[24] H. Cable, F. Laloë and W. J. Mullin, Phys. Rev. A **83**, 053626 (2011).

[25] D. Alcala, J. Glick and L. Carr, arXiv:1605.05768v1 [cond-mat.quant-gas].

[26] M. Albiez et al., Phys. Rev. Lett. **95** (2005) 010402.

[27] A. J. Leggett and A. Garg, Phys. Rev. Lett. **54**, 857 (1985).

[28] L. Rosales-Zárate, B. Opanchuk, Q. Y. He and M. D. Reid, presented at 2016 Macroscopic Entanglement Heraeus Seminar (to be published).

[29] E. G. Cavalcanti and M. D. Reid, Phys. Rev. Lett. **97**, 170405 (2006). C. Marquardt et al., Phys. Rev. A **76** 030101 (2007).

[30] E. G. Cavalcanti and M. D. Reid, Phys Rev A **77**, 062108 (2008).

[31] R. Y. Teh, L. Rosales-Zárate, B. Opanchuk, and M. D. Reid, Phys. Rev. A **94**, 042119 (2016).

[32] F. Fröwis, N. Sangouard and N. Gisin, Optics Commu-

nications **337**, 2 (2015). F. Fröwis and W. Dur, New J. Phys. **14**, 093039 (2012). P. Sekatski, N. Sangouard and N. Gisin, Phys. Rev. A **89**, 012116 (2014).

[33] E. Oudot, P. Sekatski, F. Fröwis, N. Gisin, and N. Sangouard, J. Opt. Soc. Am. B **32**, 2190 (2015).

[34] F. Frowis, P. Sekatski, W. Dur, N. Sangouard and N. Gisin, presented at 2016 Macroscopic Entanglement Heraeus Seminar. Fröwis, Florian and Sekatski, Pavel and Dür, Wolfgang Phys. Rev. Lett. **116** 090801 (2016).

[35] T. Baumgratz, M. Crammer and M. Plenio, Phys. Rev. Lett. **113**, 140401 (2014). I. Marvian and R. Spekkens, Phys. Rev. A **90**, 062110 (2014).

[36] G. K. Brennen, Quantum Inf. Comput. **3** 619 (2003). C. Bennett et al., Phys. Rev. A **53** 2046 (1996). B. Terhal and P. Horodecki, Phys Rev A **61**, 040301 (2000). J. Korsbakken et al., Phys. Rev. A **75**, 042106 (2007).

[37] S. Nimmrichter and K. Hornberger, Phys. Rev. Lett. **110**, 160403 (2013).

[38] Y. Shen et al., Phys. Rev. Lett. **114** 100403 (2015).

[39] G Svetlichny, Phys Rev D**35**, 3066 (1987). D. Collins et al., Phys. Rev. Lett. **88**, 040404 (2002). J. Lavioe et al., New J. Phys **11**, 073051 (2009). H. Lu et al., Phys. Rev. A **84**, 012111 (2011).

[40] B. Yadin and V. Vedral, Phys. Rev. A **93**, 022122 (2016).

[41] J. Esteve, et. al., Nature **455**, 1216 (2008).

[42] M. Kitagawa and M. Ueda, Phys. Rev. A **47**, 5138 (1993).

[43] D. J. Wineland, J. J. Bollinger, W. M. Itano, and D. J. Heinzen Phys. Rev. A **50**, 67 (1994).

[44] M. F. Riedel, P. Böhi, Y. Li, T.W. Hänsch, A. Sinatra and P. Treutlein, Nature (London) **464**, 1170 (2010).

[45] C. Gross et al, Nature **480**, 219 (2011).

[46] K. Maussang et al., Phys. Rev. Lett. **105**, 080403 (2010).

[47] R. Jozsa, J. Mod. Optic. **41**, 2315 (1994).

[48] H. J. Lipkin, N. Meshkov and A. J. Glick, Nucl. Phys. **62** 188 (1965).

[49] M. Steel and M. J. Collett, Phys. Rev. A **57**, 2920 (1998).

[50] Q. Y. He, M. D. Reid, T. G. Vaughan, C. Gross, M. Oberthaler and P. D. Drummond, Phys. Rev. Lett. **106**, 120405 (2011). B. Opanchuk, Q. Y. He, M. D. Reid, and P. D. Drummond, Phys. Rev. A **86**, 023625 (2012). S. Giri et al., Phys. Rev. A89, 033628 (2014).

[51] M. Egorov, et al., Phys. Rev. A **84**, 021605(R) (2011).

[52] T. Kovachy et al., Nature **528**, 530 (2015). K. S. Hardman et al., Opt. Lett. **41**, 2505 (2016).

[53] M. D. Reid, W. J. Munro and F. De Martini, Phys. Rev. A**66**, 033802 (2002).

[54] B. J. Dalton et al, arXiv:1506.06906; arXiv:1506.06892.

[55] M. Hillery and M. Zubairy, Phys. Rev. Lett. **96**, 050503 (2006).